Energy relaxation and the quasiequation of state of a dense two-temperature nonequilibrium plasma

M. W. C. Dharma-wardana*
National Research Council, Ottawa, Canada K1A 0R6

François Perrot
Commissariat a l'Energie Atomique, Boîte Postale No. 12, 91680 Bruyères-le-Châtel, France

(Received 7 January 1998)

A first principles approach to the equation of state (EOS) and the transport properties of an interacting mixture of electrons, ions, and neutrals in thermodynamic equilibrium was presented recently in Phys. Rev. E **52**, 5352 (1995). However, many dynamically produced plasmas have an electron temperature T_e different from the ion temperature T_i. The study of these nonequilibrium (non-eq.) systems involves (i) calculation of a quasiequation of state (quasi-EOS) and the needed non-eq. correlation functions, e.g., the dynamic structure factors $S_{ss'}(k,\omega)$, where s is the species index; and (ii) a calculation of relaxation processes. The energy and momentum relaxations are usually described in terms of coupling constants determining the rates of equilibriation. Simple Spitzer-type calculations of such coupling constants often use formulas obtained by averaging the damping of a *single* energetic particle by the medium. However, a different result is obtained for the energy-loss rate $\langle dH_e/dt\rangle$ of the electron subsystem when calculated from the commutator mean value $\langle[H_e,H]_-\rangle$, where H_e and H are the Hamiltonians of the electron subsystem and the total system. This result corresponds to energy relaxation via the interaction of the *normal modes* of the hot system with the *normal modes* of the cold system. Such a description is particularly appropriate for dense plasmas. The evaluation of the commutator mean values within the Fermi golden rule (FGR), or more sophisticated Keldysh or Zubarev methods, yields formulations involving the dynamic structure factors of the two subsystems. The single-particle and normal-mode methods are conceptually very different. Here we present calculations of the energy relaxation of dense uniform two-temperature aluminum plasmas, and compare the usual Spitzer-type estimates with our more detailed FGR-type results. Our results show that the relaxation rate is more than *an order of magnitude smaller* than that given by the commonly used theories. [S1063-651X(98)02309-5]

PACS number(s): 52.25.Kn, 52.25.Gj, 05.30.Fk, 71.10.−w

I. INTRODUCTION

The advent of short-pulse lasers has extended the laboratory study of nonequilibrium systems to regimes which were not accessible by standard shock-wave techniques. The shock technique enables one to heat the ions to high temperatures, while the electrons remain relatively cool since the transfer of energy from the ions to the electron subsystem is very slow. On the other hand, the laser couples strongly to the electrons and heats the electron subsystem, while the ion subsystem remains cool within the time scales appropriate to the electronic equilibriation. Thus the two experimental techniques complement each other in providing systems with cold electrons and hot ions, or hot electrons and cold ions.

The detailed thermodynamic description of an equilibrium system from *first principles* is itself a very formidable problem, since detailed atomic physics for a mixture of ionization states of ions in plasmas have to be carried out self-consistently, determining the bound states, ionization balance, equilibrium correlation functions, etc. We have recently presented such a study of the equilibrium equation of state (EOS) of Al from relatively low-temperature conditions to those of high temperatures and high compressions [1]. However, the methods to be used for determining the quasiequation of state (quasi-EOS) for a system in quasiequilibrium is not immediately evident. First of all, the meaning of the quasithermodynamic variables has to be addressed. Then their determination from a rigorous nonequilibrium technique needs to be linked with energy and momentum relaxation calculations. These are of course *not* new problems, and various classical and quantum methods, as well as simplified approaches, have been developed over the years [2,3]. Some of the modern, rigorous methods began with the work of Refs. [4,5], where it was shown how the usual S-matrix techniques can be extended to nonequilibrium problems. This method was neatly expressed by Keldysh, who presented a simple contour scheme for the implementation of the approaches of Refs. [4,5]. Developing on the ideas of Bogoliubov, Zubarev presented an extension of two-time retarded Green functions for application to nonequilibrium systems. In practice, the latter approach is harder to apply numerically, but gives an insightful understanding of the meaning of various quasithermodynamic variables in quasiequilibrium systems. The essential point is that in an equilibrium system, just as the chemical potential μ is the Lagrange multiplier for the conservation of particle number, the temperature variable ($\beta=1/k_BT$) is simply the Lagrange multiplier that expresses the conservation of the total energy (i.e., $\langle H\rangle$). It is not an expression of some ''average kinetic energy,'' etc., even though it does play that role in some model systems. When we go to a system in some quasiequi-

*Electronic mail: chandre@cm1.phy.nrc.ca

librium state, it may turn out that the energy of the electron subsystem, $\langle H_e \rangle$, is conserved for certain time scales τ_e, while the energy of the ion subsystem, $\langle H_i \rangle$, is conserved for other time scales τ_i. Under such conditions, we can introduce two Lagrange multipliers β_e and β_i to insist on the conservation of subsystem energies within their respective time scales. The interaction between the two systems, given by $H_{\rm int}$, cannot be assigned to either β_s, $s=e$ and i. Initially, when the external perturbations (e.g., the energy deposition from a laser) are switched on, the system evolves very rapidly, and it is often impossible to identify these conserved quantities. However, once a quasiequilibrium state is attained, it is possible to identify quasiconserved quantities like β_s, P_s, or Ω_s representing the pressure and the quasithermodynamic potential of the subsystem s.

In this paper we assume that the nonequilibrium evolution of the system from some initial state to some quasiequilibrium state, with given subsystem densities ρ_s and inverse temperatures β_s, has been achieved, and that their values are known. For simplicity, in this work we assume that there are just two subsystems, i.e., electrons and one kind of ion. Using the quasiequilibrium system parameters as inputs, we calculate the energy relaxation of the interacting subsystems via the traditional single-particle stopping power approach, as well as from the full many-body approach. In the latter approach it turns out that the energy relaxation occurs from the normal modes of the hot subsystem to the normal modes of the cold subsystem. Thus the calculation of the dynamic structure factors $S_e(k,\omega,T_e)$ and $S_i(k,\omega,T_i)$ of the two subsystems becomes an essential step. Another important aspect of the relaxation calculation is the ion-electron interaction potential $U_{\rm ie}$, which depends in a complicated way on the internal bound-state structure of the ions. Thus an atomic-physics problem where the electron-ion coupling as well as the ion-ion coupling is strong has to be solved to all orders, and then the necessary electron-ion pseudopotentials have to be constructed. That is, we assume that the ionization equilibrium between the bound electrons and the free electrons occur rapidly enough (compared to electron-ion equilibriation), so that the core electrons at each temperature can be projected out via the construction of the pseudopotential. Most of these steps are identical to the ones used in the equilibrium EOS calculation. [1] However, some pertinent nonequilibrium issues are addressed in Appendix A. Hence the main focus of this work is the calculation of relaxation rates. In Sec. II, we describe our two-temperature theory of a neutral, spatially uniform plasma, and assume that the ion density $\overline{\rho}$ and the effective ionic charge $\overline{Z}$, as well as the temperatures T_i and T_e of the ions and electrons are given, and that the initial source of excitation (e.g., the intense laser field) is switched off. We also assume that charge neutrality exists at least in a global sense, and hence the electron density $\overline{n}$ is such that $\overline{n}=\overline{Z}\overline{\rho}$. With these as input, we set up the calculation of the energy relaxation rate ($\dot{E}_{\rm rlx}$) using the Fermi golden rule (FGR). This calculation involves the computation of frequency dependent (i.e., dynamic) structure factors of the electron fluid and the ion fluid, using the interaction potentials obtained from the detailed microscopic description of the plasma. In the FGR approach, the two subsystems are assumed to be ''independent'' in the sense that their response functions, etc., can be calculated without reference to the dynamics of the other system, although static mean-field effects of the other system could be incorporated. The construction of the ion-ion pair potential, which involves the screening of the ions by the free electrons, is an example of such a static effect that is already included. A more sophisticated calculation includes the dynamical interaction between the two subsystems (i.e., a coupled-mode description) and this cannot be treated using the FGR, but we show that the final result, obtained using Keldysh methods, looks like a FGR result with renormalized quantities. These detailed calculations of $\dot{E}_{\rm rlx}$ are now used to compare (i) the $\dot{E}_{\rm rlx}$ predicted from a simple prescription based on the approaches of Spitzer [2], Brysk [3], and Lee and More [6].

II. THEORY

In this section we review the theory of energy relaxation within four schemes, where the first two use a *single* test particle as the starting point of the $\dot{E}_{\rm rlx}$ analysis.

(i) *Classical collisional approach:* The simplified classical approach considers the energy exchange in a binary collision, and takes an average over the distribution functions to obtain the energy-relaxation rate. Such a discussion was found by Spitzer [2]. The effects of partial electron degeneracy were treated by Brysk [3] within the same approach. Fokker-Plank-Langevin-type theory provided a more general and sophisticated treatment of this problem in terms of the friction and diffusion coefficients of a test particle in a plasma [7]. Such a general discussion has the advantage that approximations can be tested against various sum rules and conservation properties.

(ii) *Self-energy approach:* The imaginary part of the self-energy is the stopping power sometimes used for calculating energy relaxation. Hence we develop the formal expressions for the damping estimated via the self-energy, and also note the analogy with the classical Fokker-Plank method. Also, we introduce the diagrams which arise also in presenting the FGR as well as coupled-mode calculations. Here we give the formal generalization to two-temperature systems, but numerical calculations are not presented as the formal expressions derived here are enough to show the limitations of the method.

(iii) *Fermi golden rule approach:* The quantum mechanical calculation of the energy-relaxation rate of electrons (say), involves the evaluation of $\langle \dot{H}_e \rangle$, which is given by the commutator average $\langle [H_e,H]_- \rangle$, where H_e and H are the Hamiltonians for the electron subsystem and for the total system. It can be shown that this leads in the simplest approximation to the FGR calculation of the energy-relaxation rate. Here we assume that we have two ''weakly coupled'' subsystems whose response functions can be calculated independently of the dynamics of each other, and that the FGR gives the interaction rates. This is conceptually *different* from the rate calculation via single-particle kinematics, even if the two calculations lead to similar results in suitable limits. The FGR calculation of the relaxation rate uses the *mode spectrum* of the plasma, and holds in general, irrespective of whether the modes are strongly correlated and collective, or single-particle-like. Numerical results will be presented within this scheme.

(iv) *Coupled-mode energy-relaxation rate:* In this approach, we do not assume that the electron subsystem and the ion subsystem are ''independent'' to the extent that their excitations can be treated independently. That is, we include the interactions between the density fluctuations of the electron subsystem and the ion subsystem at the dynamical level. The FGR is not *a priori* applicable to systems with coupled modes. However, use of other methods (e.g., the Keldysh technique) shows that the final results have the form of a renormalized FGR. The coupled modes play the role of a hot-ion bottleneck to relaxation, and slow the relaxation in a nonlinear way, and become important for certain time scales. Numerical results for this case are also presented. Further, the last three (quantum) calculations hold in the classical regime as well and make contact with the Fokker-Plank-type approaches which are limited to the classical regime.

Although we use atomic units ($e=\hbar=m_e=1$) in this paper, sometimes m_e and other quantities will be displayed when this is helpful. Temperatures T_i and T_e will be in Hartree energy units or in eV. The effective ionic charge $\overline{Z_i}$ may sometimes be denoted by $\overline{Z}$.

A. Fokker-Plank method and simplified classical approaches

Let us first review the usual method of calculation of the energy relaxation rate of a fast particle, called a *test* particle, interacting with a set of *field* particles. The typical time scale τ_1 for the single-particle distribution functions to relax is of the order of $\sim\lambda/\overline{v}$, where λ is the mean free path and $\overline{v}$ is the mean velocity. The typical relaxation times for correlated processes involving n-body effects may be denoted by τ_n. If we consider the pair-distribution function and related plasma oscillation modes, then τ_2 is of the order of $\lambda_D/\overline{v}$, where λ_D is a screening length which becomes the Debye length in weakly correlated plasmas. As long as $\tau_1 \gg \tau_2$ etc., the single-particle collision picture can be used. But in strongly coupled plasmas, λ_D becomes comparable to mean interparticle distances, and τ_2 may no longer be small in comparison to τ_1. Thus, while the single-test-particle approach may be valid in some regimes, it should become inapplicable in sufficiently dense plasmas. In fact, the f-sum rule is essentially exhausted by the weight of the plasma peak even in dilute plasmas, and this emphasizes the inadequacy of the single-particle picture.

In the single-particle (nonquantum) approach we consider the kinetic energy w of a test particle, viz., $w=\frac{1}{2}mv^2$. Its rate of change, for a ''Brownian-like'' time scale τ, is the mean change $\langle\Delta w\rangle/\tau$ arising from the velocity change $\mathbf{\Delta v}$ during the time interval τ. The velocity changes arise from collisions and can be expressed via the friction coefficient $\mathbf{F(v)}$ and the diffusion coefficient $\mathbf{D(v)}$. Thus [7]

$$dw/dt=\frac{m}{2}\langle|\mathbf{v}+\mathbf{\Delta v}(\tau)|^2-|v|^2\rangle/\tau \tag{1}$$

$$=m\mathbf{v}\cdot\mathbf{F}(\mathbf{v})+\frac{m}{2}\mathrm{Tr}\ \mathbf{D}(\mathbf{v}), \tag{2}$$

$$\mathbf{F}(\mathbf{v})=\langle\mathbf{\Delta v}\rangle/\tau, \tag{3}$$

$$\mathbf{D}(\mathbf{v})=\langle\mathbf{\Delta v}\mathbf{\Delta v}\rangle/\tau. \tag{4}$$

The friction coefficients can be written as

$$\mathbf{F}(\mathbf{v})=\mathbf{F}_1+\mathbf{F}_2,$$

$$\mathbf{F}_1=(\overline{Z_t}^2/m)\int\frac{dk^3}{(2\pi)^3}[V(k)\mathbf{k}]\mathrm{Im}[\epsilon(\mathbf{k},\mathbf{k}\cdot\mathbf{v})^{-1}],$$

$$\mathbf{F}_2=\tfrac{1}{2}\partial\cdot\mathbf{D}(\mathbf{v})/\partial\mathbf{v},$$

and depends on the imaginary part of the dielectric function, as in the usual stopping power treatment. In the above, $\overline{Z_t}$ is the charge of the test particle. The diffusion-coefficient term can also be expressed in terms of a dielectric tensor as

$$\mathbf{D}(\mathbf{v})=\frac{2\pi\overline{Z_t^2}}{m^2}\int\frac{dk^3}{(2\pi)^3}[\overline{Z_f^2}V(k)^2\mathbf{kk}]\frac{f_f(\mathbf{v}')\,\delta[\mathbf{k}\cdot(\mathbf{v}-\mathbf{v}')]}{|\epsilon(\mathbf{k},\mathbf{k}\cdot\mathbf{v})|^2}. \tag{5}$$

This equation explicitly involves the charge $\overline{Z_f}$ and the distribution function $f_f(\mathbf{v})$ of the field particles. For the present we note that these expressions (when averaged over the particle distributions) yield an energy-relaxation rate for a system of electrons (test particles) and ions (field particles). In the high-temperature limit, the following result due to Spitzer is recovered [2]:

$$\langle dT_e/dt\rangle=-(m_e/M_i)(3/2)(T_e-T_i)/\tau_{\mathrm{ei}}^{\mathrm{rlx}}, \tag{6}$$

where

$$\tau_{\mathrm{ei}}^{\mathrm{rlx}}=\mathcal{T}^{3/2}/(8/3)\sqrt{(2\pi)}\overline{\rho}\overline{Z_i}^2\ln\Lambda, \tag{7}$$

$$\mathcal{T}=[T_e+T_i(m_e/M_i)], \tag{8}$$

$$\ln(\Lambda)=\ln(\lambda_D/\lambda_{\min}). \tag{9}$$

In these and other equations, T_i and T_e are in energy units. Z_i and M_i are the ion charge and mass, respectively. The Coulomb logarithm $\ln(\Lambda)$ involves the ratio of the average closest distance of approach, i.e., $\lambda_{\min}$ and the Debye screening length λ_D. Note that for a classical plasma of particles with no internal structure, the internal energy E_s of the species s is $\frac{3}{2}T_s$, and hence the temperature relaxation rate is essentially the same as the energy relaxation rate. But in a more general approach the internal energies of the ion subsystem and the electron subsystem in a nonequilibrium setting (i.e., quasiequations of state for each species) are needed to convert the energy-relaxation rate to the temperature relaxation rate.

The above equations, viz., Eq. (7), etc., hold in the regime where the distribution functions are completely Maxwellian. When degeneracy effects are to be taken into account [3], it is usual to write, within some approximation, the energy-relaxation rate in terms of a suitable electron-ion collision frequency $\langle\nu_{\mathrm{ei}}^{\mathrm{col}}\rangle$. Many approximate forms for $\langle\nu_{\mathrm{ei}}^{\mathrm{col}}\rangle$ are found in the literature, often with the ion temperature set to zero [8]. Here we use a generalization which reduces in the $T_i=0$ limit to the collision frequency given by Lee and More [6]. Thus

$$\overline{\tau}_{\rm ei}^{\rm col}=\frac{3T^{3/2}[1+e^{-\mu/T_e}]}{2m_e\sqrt{2}\overline{Zn}\,\ln(\Lambda)}F_{1/2}(\mu/T_e), \tag{10}$$

where

$$F_j(\eta)=\int_0^\infty t^j dt/[1+\exp(t-\eta)],$$

$$\ln(\Lambda)=\tfrac{1}{2}\ln[1+\lambda_D^2/\lambda_{\rm min}^2],$$

$$\lambda_D^{-2}=4\pi\overline{n}\{[T_e^2+(3E_F/2)^2]^{1/2}+\overline{Z}/T_i\},$$

$$\lambda_{\rm min}=\max[\overline{Z}/3T_e,h/(2\sqrt{3T_e m_e})].$$

Here the Debye length is interpolated between the Debye value and the Thomas-Fermi value, while the minimum impact parameter is either the classical distance of closest approach or the de Broglie length. Further, in Eq. (8) we have slightly modified the $T^{3/2}$ term of Lee and More to include the ion temperature T_i which is needed in the electron-ion relaxation problem. This Lee-More model and other models vary in some details but lead to similar numerical estimates (to within a factor of 2) of the relaxation rate. Hence we shall use the above equations as a representative of the conventional Spitzer-type calculation of $\dot{E}_{\rm rlx}$ inclusive of some degeneracy effects.

B. Quantum mechanical self-energy approach

The discussion of the self-energy for equilibrium systems with point ions is well known. Here we consider the case involving pseudopotentials and the two-temperature generalization of the self-energy. The single-particle electron propagator $G(\mathbf{k},t;\mathbf{k}',t')$, i.e., $\langle\langle a_{\mathbf{k}},a_{\mathbf{k}'}^{\dagger}\rangle\rangle$, describes the propagation of an electron introduced into the system (created) in the momentum state $\mathbf{k}$, at time t, and removed (annihilated) from the momentum state $\mathbf{k}'$, at time t' [9]. The propagating particle suffers scattering events, and acquires an energy shift and a damping which are given by the real and imaginary parts of the self-energy $\Sigma(\mathbf{k},\mathbf{k}')$. This is related to the noninteracting Green function G^0 and the full Green function G by the Dyson equation. A number of complications arise in dealing with nonequilibrium systems. When using the Keldysh form of the Martin-Schwinger approach, all Green functions, self-energies etc., become (2×2)-matrix operators, where G_{11} deals with propagation from time $t=-\infty$ to $t+i\epsilon$ above the real axis, and G_{22} returns the system from time $t-i\epsilon$ to $t=-\infty$ below the real axis. Thus the Dyson equation itself becomes a matrix equation. However, it turns out that, in the present problem, the results of the full analysis have the same *form* as those of the equilibrium problem, except that all the distribution functions appearing in the final result have to be the nonequilibrium ones. Hence in this section we write the normal self-energy for a system of ions at temperature T, containing electron Fermi distributions $n(k,T)$ and ion distribution functions $\rho(k,T)$, and replace them by $n(k,T_e)$ and $\rho(k,T_i)$ as appropriate. Also, in the following we replace the time interval $t'-t$ by ω via a Fourier transform, and hence assume that steady state conditions hold for time scale larger than the basic scattering times appearing in the self-energy. Further, atomic units are used in the equations:

$$G(\mathbf{k};\mathbf{k}',\omega)=G^0(\mathbf{k};\mathbf{k}',\omega)/[1+\Sigma(\mathbf{k},\mathbf{k},\omega)], \tag{11}$$

$$G^0(\mathbf{k};\mathbf{k}',\omega)=\delta(\mathbf{k};\mathbf{k}')/(\omega-\epsilon_{\mathbf{k}}), \tag{12}$$

$$\Sigma(\mathbf{k},\mathbf{k},\omega)=\int GW\Gamma\, d\xi, \tag{13}$$

$$\epsilon_{\mathbf{k}}=k^2/2. \tag{14}$$

The self-energy evaluation needs the full Green function G, the screened potential W, and the vertex function Γ. All the intermediate variables (ξ) of momentum and frequency are integrated out. Since G is unknown at the outset, in practical calculations Σ is expanded in a series of Feynman diagrams in increasing order of the *screened* interaction W and the noninteracting Green function G^0. In the equilibrium problem the S-matrix development propagates the system in its ground state at $T=-\infty$ to the ground state at $T=\infty$. In the nonequilibrium case the system need not return to the initial state when propagated to $T=\infty$ (where the interactions are asymptotically switched off). This difficulty is solved in the Keldysh method by propagating the system back to its initial state at $T=-\infty$. Further, experience has shown that useful results are obtained by taking the vertex function to be unity, leading to the GW approximation first studied in detail by Hedin for the electron gas. In our problem, the self-energy has contributions from electron-electron scattering and from electron-ion scattering. The electron-ion contribution to the self-energy is of interest to us in the energy-relaxation problem. Of course, it is not clear that a GW evaluation of Σ would be adequate in the electron-ion problem, even though it may be the case for electron gases in metals. Our approach would be to evaluate the self-energy in a generalized random-phase approximation (RPA) where realistic pair-distribution functions $g_{\rm ii}(r)$ and $g_{\rm ie}(r)$ of the ions and electrons are used instead of the simple RPA forms. The necessary all-order static distribution functions can be obtained via suitable density-functional and hypernetted-chain (HNC) methods [10]. Further, by explicitly constructing *weak* ion-electron pseudopotentials $U_{\rm ie}$ which model the all-order density-functional calculations, a first order calculation of Σ using the screened $U_{\rm ie}$ becomes quite justifiable.

The lowest order screened e-e and e-i diagrams are given in Figs. 1 and 2. Figure 1(a) is just the bare exchange diagram, while Fig. 1(b) brings in the density fluctuations in the electron gas. In the e-i case (Fig. 2), the propagating electron emits an ion-density fluctuation and reabsorbs it at a later time. The e-i interaction lines are denoted with a star at the ion vertex. This interaction is screened by electron-polarization loops (shaded loops) and ion-polarization loops (diagonally hatched loops). In fact, Fig. 2(c) corresponds to the coupled-mode case discussed in detail in Appendix B. The usual discussions [e.g., in Fokker-Plank theory, Eq. (5)] include only the screening from the electron subsystem and correspond to Fig. 2(b).

Density fluctuations are bosonlike, and their contribution is denoted Σ_B. In the e-e case the propagating electron emits and absorbs an electron-density fluctuation. It also undergoes

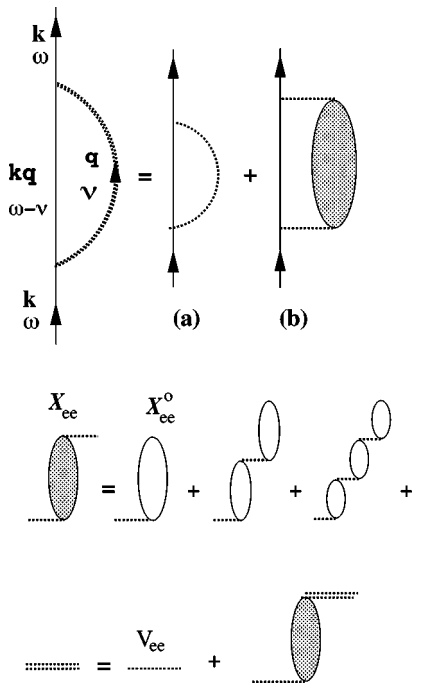

FIG. 1. The electron in the state $(\mathbf{k},\omega)$ is exchange scattered to state $(\mathbf{k}-\mathbf{q},\nu)$ by the Coulomb interaction. (a) Bare exchange interaction. (b) The Coulomb interaction is replaced by a screened interaction consisting of electron-polarization loops. In actual calculations the effect of vertex corrections (not shown in the diagrams) are approximated via local-field corrections. These diagrams are entirely in the electron subsystem, and do not contribute to energy relaxation.

exchange scattering and hence there is a Σ_x. The diagrams (at finite temperature) can be evaluated using the Matsubara rules applied separately to each subsystem, and leads to the same result (in this case) as those obtained from the Keldysh method. Then we have

$$\Sigma_{\rm ee}=\Sigma^{e}_{B}(\mathbf{K},\omega)+\Sigma^{e}_{x}(\mathbf{K},\omega), \tag{15}$$

$$\Sigma_{\rm ei}=\Sigma^{\rm ei}_{B}(\mathbf{K},\omega), \tag{16}$$

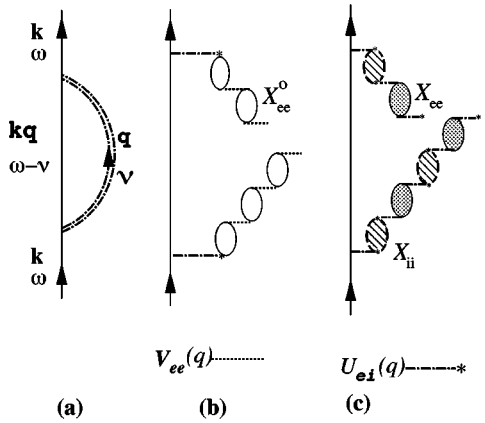

FIG. 2. The electron in state $(\mathbf{k},\omega)$ is scattered to state $(\mathbf{k}-\mathbf{q},\nu)$ by the electron-ion interaction. The ion vertex is indicated by a star. (b) shows the screening of the electron-ion interaction by the electron subsystem. (b) shows the coupled-mode behavior involving the mixing of electron polarizations and ion polarizations.

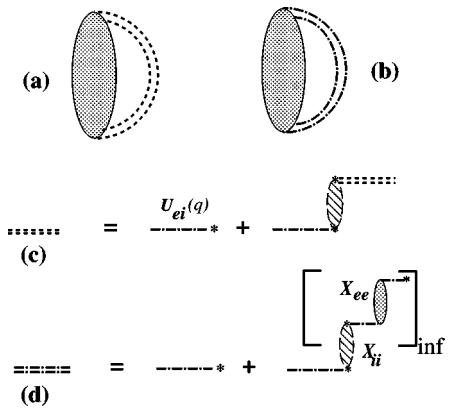

FIG. 3. (a) Feynman diagram for the lowest order energy-relaxation process corresponding to the simple Fermi golden rule. The cross-hatched oval is the electron polarization. The dot-dashed line decorated with a star is the bare electron-ion interaction. Its screening by the ion subsystem only is shown in (c). (b) Diagram for the coupled-mode energy relaxation. The doubled dot-dashed line is the renormalized electron-ion interaction given by the Dyson equation shown in (d). The diagrams have to be evaluated using the Martin-Schwinger-Keldysh rules for nonequilibrium problems [4].

$$\Sigma^{s}_{B}=\int\frac{U^{s}(q)d\mathbf{q}}{(2\pi^{3})}\int_{-\infty}^{\infty}\frac{d\omega' A^{s}(\mathbf{q},\omega')N^{s}(\omega'/T_{s})}{D(\omega,\omega')}, \tag{17}$$

$$\Sigma^{e}_{x}=-\int\frac{V(q)d\mathbf{q}}{(2\pi^{3})}\int_{-\infty}^{\infty}\frac{d\omega' A^{e}(\mathbf{q},\omega')'n_{\mathbf{k}-\mathbf{q}}}{D(\omega,\omega')}, \tag{18}$$

$$D(\omega,\omega')=(\omega+i\delta-\omega'-\epsilon_{\mathbf{k}-\mathbf{q}}), \tag{19}$$

$$A^{s}(\mathbf{q},\omega)=-A^{s}(\mathbf{q},-\omega)=-2\,{\rm Im}\chi^{s}(\mathbf{q},\omega), \tag{20}$$

$$N^{s}(\omega)=1/[\exp(\omega/T_{s})+1]. \tag{21}$$

In the above equations, $U^{s}(q)$ is the *s*-*e* pseudopotential and, hence, for *e*-*e*, this is just the bare Coulomb interaction $V(q)=4\pi/q^{2}$. The ion-electron pseudopotential $U^{i}(q)$ will be more explicitly denoted by $U_{\rm ie}(q)$, and is obtained from the full nonlinear density response of the ion in its Wigner-Seitz cavity to a uniform electron gas, calculated from the Kohn-Sham equations [1]. The equations given above are for the simpler case of Fig. 3(a). The coupled-mode form, Fig. 2(b) would require the use of the coupled mode $\chi_{\rm cm}(\mathbf{q},\omega)$ and the coupled-mode distribution function $N_{\rm cm}(\omega)$. This will be discussed in Sec. II D and in Appendix B.

The noninteracting single electron energy $\epsilon_{\mathbf{k}\text{-}\mathbf{q}}$ of the intermediate state $\mathbf{k}\text{-}\mathbf{q}$ and its occupation number $n_{\mathbf{k}\text{-}\mathbf{q}}$ occur in these equations. The bosonic spectral functions $A^{s}(\mathbf{q},\omega)$ are related to the response functions by Eq. (20), and to the dynamic structure factors by the equation

$$S^{s}(\mathbf{q},\omega)=\frac{1}{2\pi}N^{s}(-\omega)A^{s}(\mathbf{q},\omega). \tag{22}$$

We also note that since the response functions are expressible in terms of the inverse dielectric function, the spectral function term can be rewritten to explicitly show that the potentials occurring in the above expressions are the (dynamically) screened quantities. The construction of response

functions, etc., will be taken up below, in our discussion of the dynamic structure factors. At this juncture we note that the self-energy equations describe the damping of the propagating electron occurs via its scattering with the *normal modes* of the system, and not in terms of simple binary collisions.

Since we are interested in the damping rate due to electron-ion interactions, the quantity of interest is the imaginary part of $\Sigma_B^{\rm ei}$. This can be finally written in terms of a single-particle electron-ion collision time τ^{Σ} as follows:

$$1/\tau(k)^{\Sigma_{\rm ie}} = -2\ {\rm Im}\Sigma^{\rm ei}. \tag{23}$$

However, we are not interested in the number of collisions, but in the energy-relaxation rate $\dot{E}_{\rm rlx}$. $\dot{E}_{\rm rlx}$ for an electron of energy $\omega = k^2/2$ and momentum $\mathbf{k}$ is obtained by including a factor of ω' inside the $d\omega'$ integration in Eq. (17). To obtain the energy loss from the whole electron subsystem, it would at this stage be natural to average over the electron distribution. Thus the one-electron self-energy approach would lead us to the estimate for $\dot{E}_e$ given by

$$\dot{E}_e^{\Sigma} = \int \frac{dk^3}{(2\pi)^3} n(k,T_e)\,\gamma(k,T_e), \tag{24}$$

$$\gamma(k,T_e) = \int \frac{dq^3}{(2\pi)^3} |V_{\rm ei}(q)|^2 \int d\omega'\,\omega' f(\omega',\mathbf{k},\mathbf{q}], \tag{25}$$

where

$$f(\omega',\mathbf{k},\mathbf{q}) = \delta(\omega-\omega'-\epsilon_{\mathbf{k}-\mathbf{q}}) N(\omega'/T_i) A^i(q,\omega').$$

Note that in the above expressions, the electron and ion-distribution functions contain their respective subsystem temperatures T_e and T_i.

C. Fermi golden rule approach

In the classical Fokker-Plank approach and the quantum self-energy approaches, the damping of a *single* test-particle was calculated first, and then an average over the test-particle distribution was used to obtain the overall relaxation rate. However, quantum mechanically, the energy-relaxation rate of a subsystem with the Hamiltonian H_s is essentially $\langle \dot{H}_s \rangle$, and this is given by the commutator mean value $\langle [H_s, H] \rangle$, where H is the total Hamiltonian. In this problem (as well as in the previous two approaches), the nature of the nonequilibrium density matrix used in the calculation of the mean value has to be resolved. However, as discussed in Appendix A, once quasiequilibrium conditions are assumed, the state functions of each subsystem (at its quasiequilibrium density and temperature) are easily calculated. Then the lowest order evaluation of $\langle [H_s, H] \rangle$ reduces to a FGR calculation of the energy-exchange rate between the two subsystems. The diagrammatic content of the calculation is shown in Figs. 3(a) and 3(c), and should be compared with Figs. 1 and 2, which define the self-energy calculation.

The electron-ion interaction Hamiltonian is given by

$$H_{\rm ei} = \sum_{\mathbf{k},\mathbf{k}',\mathbf{q}} U_{\rm ie}(\mathbf{q}) a_{\mathbf{k}}^{\dagger} a_{\mathbf{k}'} \tilde{\rho}_{\mathbf{q}}, \tag{26}$$

$$\tilde{\rho}_{\mathbf{q}} = [\rho_{\mathbf{q}} + \rho_{-\mathbf{q}}^{\dagger}]. \tag{27}$$

Here $\rho_{\mathbf{q}} = \Sigma_{ij} e^{i\mathbf{q}\cdot(\mathbf{r}_i - \mathbf{r}_j)}$ defines an ion-density fluctuation with wave vector $\mathbf{q}$. Also, $\mathbf{r}_i$ and $\mathbf{r}_j$ are ion coordinates. To simplify the presentation, we assume for the moment that the spectral function $A(\mathbf{q},\omega)$ describing ion density fluctuations has essentially one mode at $\omega_{\mathbf{q}}$, e.g., the plasmon mode. The full mode spectrum will be restored in the final results. Let the electron subsystem go from the initial state $\mathbf{k}'$ to the final state $\mathbf{k}$, whereby the ion subsystem increases its population of density fluctuations from $N(\omega_q/T_i)$ in the initial state to $N(\omega_q/T_i)+1$ in the final state. Here $N(\omega_q/T_i)$ is a Bose factor at temperature T_i, and will be abbreviated by $\overline{N_q^i}$. We denote the probability of this process by $W^{\uparrow}$, and have

$$W^{\uparrow} = 2\pi |U_{\rm ie}(q)\,\alpha_{k,k'}(q)|^2 \delta_{k,k'}^{-}(q), \tag{28}$$

$$\alpha_{k,k'}(q) = \langle k, N_q^i + 1 | a_{\mathbf{k}}^{\dagger} a_{\mathbf{k}'} \tilde{\rho}_{\mathbf{q}} | \mathbf{k}', N_q^i \rangle, \tag{29}$$

$$\delta_{k,k'}^{-}(q) = \delta(\epsilon_{\mathbf{k}'} - \epsilon_{\mathbf{k}} - \omega_{\mathbf{q}}). \tag{30}$$

This further reduces to

$$W^{\uparrow} = 2\pi |U_{\rm ie}(q)\,\eta_{k,k'}(\mathbf{q})|^2 (\overline{N_q^i}+1)\,\delta_{k,k'}^{-}(q). \tag{31}$$

Here $\eta_{k,k'}(\mathbf{q})$ denotes a density fluctuation in the electron subsystem arising from the transition of the electron from state $\mathbf{k}'$ to state $\mathbf{k}$, with the emission of momentum $\mathbf{q}$. Similarly we have a rate $W^{\downarrow}$ for the opposite process:

$$W^{\downarrow} = 2\pi |U_{\rm ie}(q)\,\eta_{k,k'}(\mathbf{q})|^2 \overline{N_q^i}\,\delta_{k,k'}^{+}(q), \tag{32}$$

$$\delta_{k,k'}^{+}(q) = \delta(\epsilon_{\mathbf{k}'} - \epsilon_{\mathbf{k}} + \omega_{\mathbf{q}}). \tag{33}$$

Thus the energy exchange rate $\dot{E}_{\rm rlx}$ is

$$\dot{E}_{\rm rlx} = 2\pi\Sigma\,\omega_{\mathbf{q}} |U_{\rm ie}(q)\,\eta_{k,k'}(\mathbf{q})|^2 \mathcal{P}_{\mathbf{k}'} [\{\overline{N_q^i}+1\}\delta^{-} - \delta^{+}(\overline{N_q^i})].$$

Here $\mathcal{P}_{\mathbf{k}'}$ is the statistical probability of occurrence of the initial electronic state $\mathbf{k}'$. We interchange the dummy indices $\mathbf{k}$ and $\mathbf{k}'$ in the last delta function, and use the fact that

$$\epsilon_{\mathbf{k}'} = \epsilon_{\mathbf{k}} + \omega_{\mathbf{q}}, \quad P_{\mathbf{k}} = P_{\mathbf{k}'} e^{(\omega_{\mathbf{q}}/T_e)} \tag{34}$$

to write $\dot{E}_{\rm rlx}$ in the form

$$\dot{E}_{\rm rlx} = 2\pi\Sigma\,\omega_{\mathbf{q}} |U_{\rm ie}(q)\,\eta_{k,k'}(\mathbf{q})|^2 [(\overline{N_q^i}+1) - e^{(\omega_{\mathbf{q}}/T_e)} \overline{N_q^i}]$$
$$\times \sum_{\mathbf{k},\mathbf{k}'} |\eta_{k,k'}(\mathbf{q})|^2 \mathcal{P}_{\mathbf{k}'}\,\delta(\epsilon_{\mathbf{k}'} - \epsilon_{\mathbf{k}} - \omega_{\mathbf{q}}).$$

The electron-response function can be written in the form

$$\chi_{\rm ee}(,\mathbf{q},\omega)=\sum_{\mathbf{k},\mathbf{k}'}\frac{|\eta_{k,k'}(\mathbf{q})|^2(\mathcal{P}_{\mathbf{k}'}-\mathcal{P}_{\mathbf{k}})}{\omega+i\delta+\epsilon_{\mathbf{k}'}-\epsilon_{\mathbf{k}}}$$

$$=(e^{\omega/T_e}-1)\sum_{\mathbf{k},\mathbf{k}'}\frac{|\eta_{k,k'}(\mathbf{q})|^2\mathcal{P}_{\mathbf{k}'}}{[\epsilon_{\mathbf{k}'}-\epsilon_{\mathbf{k}}-(\omega+i\delta)]}.$$

The quantity $(e^{\omega/T_e}-1)$ is simply the reciprocal of the Bose factor $N(\omega/T_e)$ at the *electron* temperature. Hence, rewriting the expression for $\dot{E}_{\rm rlx}$ in terms of Im $\chi_{\rm ee}(q,\omega)$ and simplifying, we have

$$\dot{E}_{\rm rlx}=\Sigma_{\mathbf{q}}\omega_{\mathbf{q}}|U_{\rm ie}(q)|^2[N(\omega_{\mathbf{q}}/T_e)-N(\omega_{\mathbf{q}}/T_i)]A^e(q,\omega_q). \tag{35}$$

Up to now we have assumed that the ion-density fluctuation spectral function is of the delta-function form $-2\pi[\delta(\omega-\omega_{\mathbf{q}})-\delta(\omega+\omega_{\mathbf{q}})]$. Generalizing to the full spectral function A^i given by Eq. (20), we can write $\dot{E}_{\rm rlx}$ as an integral over ω over the range $-\infty$ to $+\infty$. Using the antisymmetry properties of the spectral functions, etc., the integration range can be reduced to the range 0 to ∞:

$$\dot{E}_{\rm rlx}=\int_0^\infty\omega\frac{d\omega}{2\pi}\int\frac{dq^3}{(2\pi)^3}|U_{\rm ie}(\mathbf{q})|^2\Delta N_{\rm ei}A^eA^i, \tag{36}$$

$$\Delta N_{\rm ei}=[N(\omega/T_e)-N(\omega/T_i)], \tag{37}$$

$$A^eA^i=\{-2\ {\rm Im}\chi_{\rm ee}(q),\omega,T_e\}\{-2\ {\rm Im}\chi_{\rm ii}(q,\omega,T_i)\}. \tag{38}$$

Thus, when the electrons are hot, $\dot{E}_{\rm rlx}$ is the net energy-loss rate from electrons, and corresponds to $\langle\dot{H}_e\rangle$. If we return to the single (ion-density fluctuation) mode result [Eq. (35)], and consider the case of a solid, then it describes the energy exchange between electrons and a phonon mode of energy ω_q and reduces to Kogan's formula [11]. However, in our case the ion-density fluctuations are excitations screened by the electron fluid, and hence the ion plasmon is replaced by an acousticlike mode and other features which are best described by the full spectral function A^i. Calculation of the spectral functions needed in Eq. (36) are treated below in a separate subsection.

Coupling constants and relaxation times

The final form of the FGR expression, Eq. (36) shows that the relaxation rates are proportional to the population imbalance $[N(\omega/T_e)-N(\omega/T_i)]$ in each *mode*. Thus a mode relaxation time $\tau_{q\omega}$ can be defined such that the rate of relaxation of a given mode is given by the rate equation:

$$R_{q\omega}=\frac{[N(\omega/T_e)-N(\omega/T_i)]}{\tau_{q\omega}}, \tag{39}$$

$$\tau_{q\omega}=1/[|U_{\rm ie}(\mathbf{q})|^2A^e]. \tag{40}$$

We also note that in the limit where the temperatures are larger than any of the mode energies, $N(\omega/T)$, tends to T/ω. Hence the term (T_e-T_i) can be taken out of the summation to define a coupling constant $\overline{g}_{\rm cc}$. Thus

$$\overline{g}_{\rm cc}=\dot{E}_{\rm rlx}/(T_e-T_i), \tag{41}$$

$$\overline{g}_{\rm cc}\rightarrow\int_0^\infty\frac{d\omega}{2\pi}\int\frac{dq^3}{(2\pi)^3}|U_{\rm ie}(\mathbf{q})|^2A^eA^i, \tag{42}$$

where the last result is the limiting form. This form [Eq. (41)] has often been used in analyzing experimental data, together with the added assumption that $\overline{g}_{\rm cc}$ is a constant within the parameter space of the experiment. In such cases the energy relaxation per unit mass of matter, or per unit volume is relevant. Note that $\dot{E}_{\rm rlx}$ itself can be specified as a rate for the whole system, per ion, per electron, per unit volume, or per unit mass, as may be convenient, since we may assume that the plasma has length scales significantly larger than an electron mean free path. This assumption may not be valid for dense plasmas formed in semiconductor nanostructures. The conversion between different ways of specifying the coupling constant is not always simple. For example, a conversion between $\overline{g}_{\rm cc}$/ion and $\overline{g}_{\rm cc}$/electron requires an evaluation of the ionization balance which gives $\overline{Z}$.

D. Energy relaxation in a system with coupled modes

If we consider an ion of nuclear charge Z with effective ionic charge $\overline{Z}$, the ion carries $n_b=Z-\overline{Z}$ bound electrons. The nucleus and its n_b bound electrons are at the ionic temperature T_i. This ion is also screened by a charge displacement Δn of electrons which integrate to $\overline{Z}$. This sheath of screening electrons is at the electronic temperature T_e and adiabatically follows the ion, to within the Born-Oppenheimer approximation. This object, consisting of the nucleus, the bound electrons, and the static sheath of screening electrons, constitutes the neutral pseudoatom (NPA). Thus the NPA is a two-temperature object, with the nucleus and the inner core at T_i, while the screening sheath is at T_e. It is this screening which converts the ion-plasmon mode at T_i into a *two-temperature* ion-acoustic mode.

In applying the FGR, it was assumed that the electron subsystem was *constructed* to be independent of the ion subsystem. This is indeed possible in a mean-field *static* sense. Thus the ion-ion pair potential was constructed to include the existing screening effects of the electrons, and this gave rise to the static ion-distribution which existed when the laser pulse arrived to heat the electrons, while the ion cores remained cold. If the coupling of the electron density fluctuations $n(q)=\Sigma_{\mathbf{k}}a^\dagger_{\mathbf{k}+\mathbf{q}}a_{\mathbf{k}}$ with the ion-density fluctuations $\rho(q)$ become dynamically important, we need a detailed coupled-mode description of the system. In such a system we do not have purely electronic or ionic normal modes, and then the energy transfer occurs from the hot modes to the cooler coupled modes of the system. Coupled-mode formation has its own time scales, and hence may not be relevant to very short-pulsed excitation processes, at least in the initial stages of the time evolution. When coupled modes are formed, electronic density fluctuations mix with ion-density fluctuations and hence the ion-mode population $N(\omega)$ is not simply $N(\omega/T_i)$ and has to be determined by two coupled processes. These are (i) electron-ion energy exchange, and (ii) a return to equilibrium of the ion populations due to the damping of

the ion modes and their coupling to the rest of the material which acts as a heat sink. The latter involves a simultaneous solution of a heat-flow equation controlling ion equilibriation. To simplify the discussion, in the following analysis we assume that the ion equilibriation is efficiently coupled so as to maintain the ion subsystem at T_i, and that coupled modes are formed without time scale restrictions. The latter assumption is in any case necessary as we do not at present have a clear picture of the time scales which determine coupled-mode effects. The theory of coupled-mode relaxation is at present a leading edge of research and controversy [23]. In order to understand the coupled-mode problem let us look at the density fluctuations in the ion subsystem. The ion-response function of the ion subsystem alone is of the form

$$\chi_{\rm ii}(q,\omega)=\chi^0_{\rm ii}/[1-V_{\rm ii}(1-\mathcal{G}_{\rm ii})\chi^0_{\rm ii}], \tag{43}$$

where $\mathcal{G}_{\rm ii}(\omega)$ is a local-field factor. When the ion-density fluctuations couple with the electron-density fluctuations, the coupled-mode function is given by the Dyson equation

$$\chi_{\rm cm}(q,\omega)=\chi_{\rm ii}/[1-\{|V_{\rm ie}(q)|^2\chi_{\rm ee}\}\chi_{\rm ii}]. \tag{44}$$

The Dyson equation iterates the ion-response loop and the screened-electron ion interaction [see Fig. 3(d)] to give the coupled-mode (cm) response function $\chi_{\rm cm}(q,\omega)$. This cm response function can be rewritten in terms of χ^0 and the e-e, i-i denominators to reveal the denominator

$$D_{\rm cm}=D_{\rm ee}D_{\rm ii}-|V_{\rm ie}(q)|^2\chi^0_{\rm ee}\chi^0_{\rm ii}, \tag{45}$$

where the denominators are

$$D_{\rm ee}=[1-V_{\rm ee}(k)(1-\mathcal{G}_{\rm ee})\chi^0_{\rm ee}],$$

$$D_{\rm ii}=[1-V_{\rm ii}(k)(1-\mathcal{G}_{\rm ii})\chi^0_{\rm ii}].$$

In fact, if a two-fluid description had been used from the outset, the ion-ion response function comes out to be of the form

$$\chi_{\rm ii}=\chi^0_{\rm ii}[1-V_{\rm ee}(k)(1-\mathcal{G}_{\rm ee})\chi^0_{\rm ee}]/\mathcal{D},$$

where the denominators are

$$\mathcal{D}=D_{\rm ee}D_{\rm ii}-D_{\rm ei},$$

$$D_{\rm ei}=|V_{\rm ei}|^2\chi^0_{\rm ii}\chi^0_{\rm ee}(1-\mathcal{G}_{\rm ie})(1-\mathcal{G}_{\rm ei}).$$

The dynamical equivalent of the local-field factors are the vertex corrections which can be formally included in the Dyson equation. In effect, $\mathcal{D}$ is simply $D_{\rm cm}$ inclusive of local-field factors. The main point about the denominator $D_{\rm cm}(q,\omega)$ is that it replaces individual density fluctuation modes ω^s_q, $s=e$ and i by hybrid modes, some of which are electronlike in one extreme, and unscreened-ion-like in the other extreme. The distribution function of this cm system is neither at T_e or at T_i. It is not a Bose, Fermi, or Maxwell distribution, but has the two-temperature form (see Appendix B)

$$\overline{N}_{\rm cm}(\omega/T_i,\omega/T_e)=\frac{\overline{N}(\omega/T_i)A^i(q,\omega)+\overline{N}(\omega/T_e)A^e(q,\omega)}{A^i(q,\omega)+A^e(q,\omega)}. \tag{46}$$

It turns out (see Appendix B) that the new expression for the energy relaxation rate in the coupled-mode picture is almost like the simple FGR result. Thus

$$\dot{E}_{\rm rlx}=\int_0^\infty\omega\frac{d\omega}{2\pi}\int\frac{dq^3}{(2\pi)^3}|U_{\rm ie}(q)|^2\Delta N_{\rm cm}A^iA^e_{\rm cm}, \tag{47}$$

$$A^e_{\rm cm}=-2\,{\rm Im}\chi_{\rm cm}(q,\omega,T_i,T_e), \tag{48}$$

$$\Delta N_{\rm cm}=N(\omega/T_e)-N_{\rm cm}(\omega/T_i,\omega/T_e). \tag{49}$$

This equation can be cast into a form which is more symmetrical in electrons and ions by rewriting it in the form

$$\dot{E}_{\rm rlx}=\int_0^\infty\omega\frac{d\omega}{2\pi}\int\frac{dq^3}{(2\pi)^3}|U_{\rm ie}(\mathbf{q})|^2\frac{\Delta N_{\rm ei}A^iA^e}{|1-\{|V_{\rm ie}(q)|^2\chi_{\rm ee}\}\chi_{\rm ii}|^2}. \tag{50}$$

Here the coupled-mode distribution has disappeared. Instead, a new denominator which is the denominator of the cm Dyson equation, Eq. (45) has taken over the job of screening the bare interactions and distribution functions.

1. Dynamic structure factors

In our application of the Fermi golden rule, we have treated the electron subsystem and the ion subsystem as two weakly interacting systems coupled via the weak pseudopotential $U_{\rm ie}$. Hence if we assume that the electron response function and the ion response function can be modeled independently, then we would have, with $s=e$ or i,

$$\chi_{ss}=\chi^0_{ss}(q,\omega,T_s)/D_{ss}, \tag{51}$$

$$D_{ss}=[1-V_{ss}(q)(1-\mathcal{G}_{ss})\chi^0_{ss}]. \tag{52}$$

Here $\chi^0_{\rm ee}$ is the Lindhard response function while $\chi_{\rm ii}$ is its classical limit usually called the Vlasov plasma-dispersion function. The finite temperature *static* electron–local-field factor $\mathcal{G}_{\rm ee}$ is available from the finite-temperature electron-exchange correlation function and related studies [12]. In the case of the ion-response function, it is very important to model the local fields, etc., so as to recover the realistic static structure factor $S_{\rm ii}(q)$ of the ion subsystem. Of course, one may construct more sophisticated dynamic structure factors (at least for the ions) by appealing to other methods based on renormalized kinetic theory of fluids, etc. However, we have found the simple methods used here to be adequate for a wide class of plasma problems. A discussion of this aspect and comparison of the dynamic ion-structure factor with that obtained by molecular dynamics simulations was given in Ref. [13]. To this end, we define $\mathcal{F}_{\rm ii}(q)$ in the following ways:

$$\chi_{\rm ii}=\frac{\chi^0_{\rm ii}(q,\omega,T_i)}{1-\mathcal{F}_{\rm ii}(q)\chi^0_{\rm ii}(q,\omega,T_i)}, \tag{53}$$

$$\mathcal{F}_{ii}(q) = 1/\chi_{ii}^{0} + T_i/[\overline{\rho} S_{ii}(q)]. \tag{54}$$

The last equation holds for the static case $\omega = 0$ when χ_{ii} is $-\overline{\rho} S_{ii}(q)/T_i$ for a classical system. The required $S_{ii}(q)$ is obtained from an HNC equation using the pair potential

$$U_{ii}(q) = \overline{Z}^2 V(q) + |U_{ie}(q)|^2 \chi_{ee}(q, T_e). \tag{55}$$

Here the (static) electron response χ_{ee} and the ion-electron pseudopotential (see Sec. II D 2) appear.

Once the dynamical χ_{ee} and χ_{ii} described so far are calculated, a reasonable approximate description of the coupled-mode forms can be constructed using the ion-electron pseudopotentials in Eq. (44). However, it should be noted that some *static aspects* of the coupled modes is already included in the FGR approach which uses dynamic structure factors constructed from the experimental (or HNC-type) static ion-ion structure factor. The dynamical coupled-mode effects play a role in various situations; e.g., they manifest themselves as ion-dynamical effects in determining the shapes of spectral lines near the line center.

2. Ion-electron pseudopotential

Once $\overline{Z}$ is available at a given ion density fixed by R_{WS} and T_e, we need the ion-electron pseudopotential U_{ie} for that electron density and temperature. A pseudopotential allows us to replace the full atomic potential by a simpler potential which deals only with a limited set of electrons, the so-called valence electrons, $\overline{Z}$ in number, and formally factorize out the core electrons attached to each nucleus. Depending on the application considered, U_{ie} may be chosen to satisfy a class of desirable properties accurately. Thus we may require that (i) the pseudopotential U_{ie} generates the same displaced charge density $\Delta n(k)$ as the full atomic potential; (ii) that it be sufficiently weak so that $\Delta n(k)$ is obtained within linear response; and (iii) that it has the same phase shifts as the original atomic problems, at least for a given range of energies. If the phase shifts are to be correctly reproduced, a nonlocal, energy-dependent pseudopotential which is not necessarily weak (in the linear response sense) becomes necessary. In such circumstances, it is often easier to work directly with the phase shifts and the relevant T matrices. Alternatively, we may choose the pseudopotential to reproduce a specific property, e.g., (a) the electrical resistivity or (b) selected peaks in the optical absorption spectrum. In this paper we will study two models for the pseudopotential, viz., a ''charge-density-fitted'' (CDF) pseudopotential, which satisfies the criteria (i) and (ii) listed above, and a ''static-resistivity fitted'' (SRF) potential, which satisfies (a). Unlike the CDF potential, which fits $\Delta n(q)$ for a full range of q values, the SRF potential is a fit to just one number (or a few numbers) and is of limited microscopic significance.

A CDF pseudopotential U_{ie} which satisfies (i) and (ii) is actually a byproduct of the density-functional calculation, and is given by

$$U_{ie}(k) = -\Delta n(k)/\chi_{ee}(k). \tag{56}$$

The displaced electron charge $\Delta n(k)$ appearing above is the *nonlinear* charge pileup around the ion of effective charge $\overline{Z}$ obtained from the density-functional procedure. Thus, since $\chi_{ee}(k)$ is the *linear* response function, $U_{ie}(k)$ is by construction a pseudopotential which gives the true nonlinear free-electron distribution in a linear response. Such a construction does not imply that the phase shifts of the pseudopotential U_{ie} are the same as that of the full atomic potential.

TABLE I. Charge-density-fitted ion-electron pseudopotentials for Al ions as a function of temperature (eV) in a plasma at the melting-fluid density ($R_{WS} = 3.121$ a.u.), i.e., unit compression. The well-depth parameter D, the pseudocore radius R_c, and the parameters λ and q_0 are defined in Eq. (60), and are in atomic units.

T (eV)	$\overline{Z}$	R_c	D	λ	q_0
2.5	3.0004	1.5417	0.7228	1.08	1.28
5.0	3.0004	1.5419	0.7687	1.26	1.40
10.0	3.0230	1.5397	0.8862	1.97	2.04
20.0	3.5997	1.4864	1.0010	3.56	3.85
30.0	4.3479	1.4479	1.0801	3.35	3.37
40.0	5.1927	1.4153	1.2480	1.35	1.31

Since we are studying a collisional property related to transport, we also consider the SRF pseudopotential determined so that the mean free path calculated using $U_{ie}(k)$ in the Ziman formula is identical to that given from the T-matrix form of the Ziman formula which uses the full atomic phase shifts from the density-functional calculation. That is, we require that

$$f_T = \int_0^\infty d\varepsilon \frac{dn_{FD}(\varepsilon)}{d\varepsilon} \int_0^{q_m} q^3 T(q) S_{ii}(q) dq, \tag{57}$$

$$f_{pseu} = \int_0^\infty \frac{q^3 \Sigma(q) S_{ii}(q) dq}{[1 + \exp\{\beta[\varepsilon(q)/4 - \mu]\}]}, \tag{58}$$

$$f_T = f_{pseu}. \tag{59}$$

In the above, $n_{FD}(\varepsilon)$ is the Fermi-Dirac occupation number for a level of energy ε. The energy ε determines the upper limit of the momentum transfer q_m for the q integration to be $(2/\hbar)\sqrt{2m\varepsilon}$. The T matrix $T(q)$ is the elastic scattering cross section (ESCS) calculated from the density-functional phase shifts [15], while $\Sigma(q)$ is the ESCS calculated from the local pseudopotential whose parameters are adjusted to ensure that f_T is equal to f_{pseu}.

Rather than using a numerical table that would result from, say Eq. (56), the CDF pseudopotentials were fitted to the forms

$$U_{ie}(k) = -V(q)\overline{Z}[DJ(qR_c) + (1 - D)\cos(qR_c)]K(q),$$

$$J(x) = \sin(x)/x, \tag{60}$$

$$K(q) = [1 + \lambda(q/q_0)^2]/[1 + (q/q_0)^2].$$

Here D is a well-depth parameter and R_c is a cutoff radius, while λ and q_0 provide additional adjustments to the q dependence of the basic Ashcroft form. Some examples of the pseudopotentials used in this work are given in Table I. In parametrizing the SRF potential, we used only the bare Ash-

croft form [i.e., $K(q)=1$], but introduced an electron effective mass m_e^* into the screening function defining the ESCS, viz., $\Sigma(q)$ appearing in Eq. (58), as in Ref. [16].

III. CALCULATIONS

In this section we present our numerical calculations for the energy-loss rate from a subsystem of hot electrons interacting with a subsystem of cold ions. Such a plasma can be generated using short-pulse laser techniques, where the pulse duration is smaller than the relevant time scales of the ions. Thus the conditions can be arranged so that the ions remain essentially near the melting temperature of the material almost at solid density, while the electrons absorb energy and reach extremely high temperatures. The properties of such a highly nonequilibrium system can be probed using a weak probe laser applied within a succession of time delays. Many such experiments have been reported, especially for Al, in the recent literature [14]. Hence we present calculations for a two-temperature Al plasma, where the ions are essentially at the melting point (943 K, 0.0813 eV) and at a density of 2.374 g/cc. This corresponds to a Wigner-Seitz (WS) radius $R_{\rm WS}$ of 3.121 a.u. (while the room temperature $R_{\rm WS}$ is 2.98228 a.u.). Thus T_i is 0.0813 eV, and T_e can be increased by raising the amount of energy deposited by the laser pulse. As T_e is increased, the heated dense electrons interact with the core electrons, and the effective ionization $\overline{Z}$ increases upwards from the value of $\overline{Z}=3$ at the melting. We calculate $\overline{Z}$ by immersing an Al nucleus together with its Wigner-Seitz cavity in an electron gas at the required temperature T_e, and self-consistently solving a Mermin-Kohn-Sham problem [10]. An ion temperature does not directly enter into this problem at this stage of the analysis, except via the choice of the Wigner-Seitz radius which depends on the ion density. No formal problem associated with the question of the applicability of density functional theory to a nonequilibrium setting arises in this calculation. Some values of the calculated $\overline{Z}$ is given in Table I. Once $\overline{Z}$ is known, the electron density $\overline{n}$ at T_e is simply $\overline{Z}\rho$, and the electron-sphere radius r_s is $R_{\rm WS}/\overline{Z}^{1/3}$.

The numerical calculations require the two dynamic structure factors $S_e(k,\omega,T_e)$ and $S_i(k,\omega,T_i)$. The dynamic structure factor of the electron subsystem is immediately available from the imaginary part of $\chi_{\rm ee}(k,\omega,T_e)$ using the temperature-dependent local-field corrections obtained from the derivative of the finite-temperature exchange-correlation potential $V_{\rm xc}(r_s,T_e)$ of density-functional theory [12]. Figure 4 shows $S_e(k,\omega,T_e)$ at 20 eV. As expected, the electron-plasma mode is well defined for small wave vectors, and broadens out for large momenta. In calculating $S_i(k,\omega,T_i)$ we first construct the *static* $S(k)$ of the ions using the ion-ion pair potential $U_{\rm ii}(k,T_i)$ obtained from $U_{\rm ie}(k,T_i)$ using Eq. (55). Thus the electron temperature T_e *does not* enter here, since the ion subsystem has not come to the temperature of the electrons, but was formed when the system was initially in equilibrium at the temperature of the ions, T_i. The static $S(k)$ is calculated using a hypernetted-chain procedure inclusive of a bridge term, for a fluid in equilibrium at T_i. This calculated $S(k)$ of liquid Al at its melting point agrees very well with the experimental $S(k)$ of Refs. [17,16]. The next step in the calculation is to use Eq. (53) to obtain the dynamic structure factor of the ion subsystem. The results of this calculation are shown in Fig. 5. The figure shows how the bare ion-plasma frequency is converted to a lower-energy ion-acoustic mode which depends nearly linearly on the wave vector. As expected, the width (damping) of the mode also increases with the value of k.

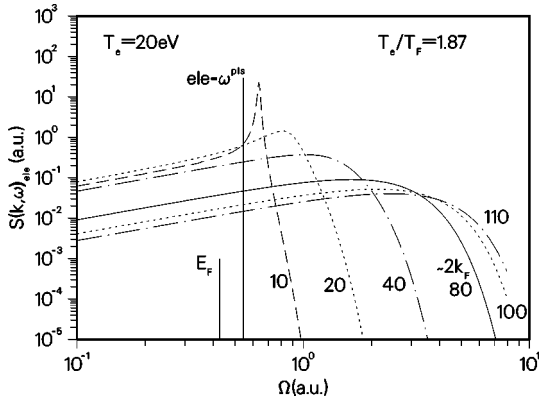

FIG. 4. The dynamic structure factor $S_e(k,\omega,T_e)$ of the electron subsystem at 20 eV. The different curves are for indicated values of the wave vector k in units where $2k_F$ is 80. The electron plasma frequency $\omega_{\rm pl}^2=4\pi\overline{n}/m_e$ is also shown. The Fermi energy is E_F.

Using these results and Eqs. (36) and (50), we can calculate the energy-relaxation rates within the simple FGR and also for the coupled-mode approach. The Spitzer-Brysk-type result [Eq. (10)] is easily calculated, and does not require the dynamic structure factors and other machinery that we have set up. Figure 6 displays the energy-relaxation rates calculated from these equations as a function of electron temperature T_e, while the ion temperature remains fixed at the melting point of liquid Al. The Spitzer-Brysk curves are about two orders of magnitude higher than the FGR estimate, which is also about an order of magnitude higher than the system with coupled modes. The energy-loss rate (ELR) calculated using the CDF pseudopotentials is shown as a solid line, while the results of the SRF pseudopotential are shown as a dashed line. These results show that the CDF and SRF approaches are in satisfactory agreement. Hence we feel that

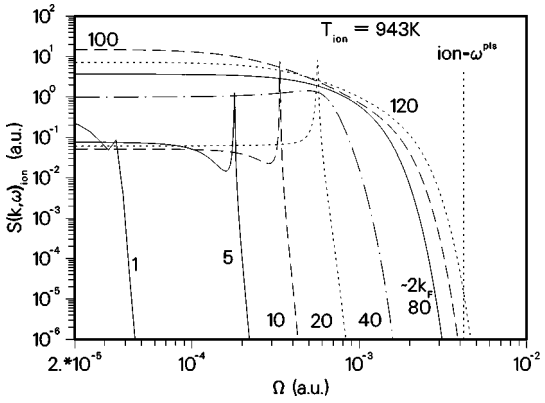

FIG. 5. The dynamic structure factor of the ion subsystem, i.e., $S_i(k,\omega,T_i)$, is shown as a function of ω and k. The bare-ion plasma frequency is also shown for comparison. T_i is the melting point (m.pt) temperature, 0.081 eV.

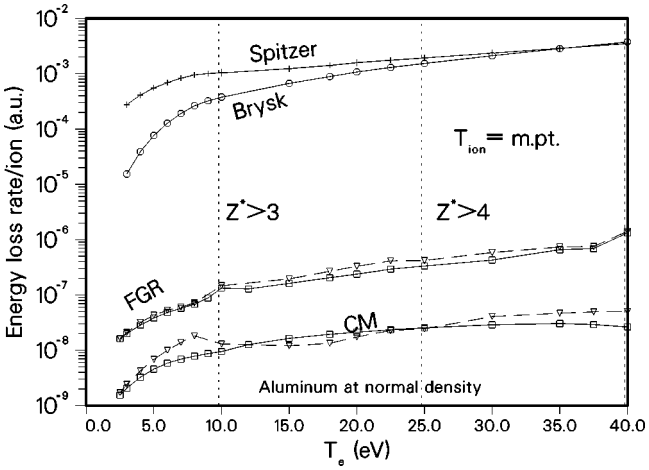

FIG. 6. The energy-relaxation rate (atomic units) calculated from various models. The curve labeled FGR is the Fermi golden rule calculation, Eq. (36). The coupled-mode calculation Eq. (50) is labeled CM. The solid and dashed lines are the results from the CDF and SRF pseudopotentials. The Spitzer-Brysk-type curve is based on a form of the collision frequency [Eq. (10)], which reduces to that of Lee and More if $T_i = 0$. The value of the effective ionic charge $\overline{Z}$ applicable to various regimes is also indicated.

the ion-electron interaction potentials are adequately handled, and that a full phase-shift approach is probably not necessary. The coupling constants corresponding to the ELR are given in Table II, and show the same strong difference between the FGR-type results and the estimate from the Spitzer-Brysk approach. The even greater slowing down of the relaxation rate under coupled-mode formation is what one would expect on simple physical grounds. One might associate a ''temperature'' $T_{\rm mode}$ for each mode, using the distribution given in Eq. (46) by writing

$$\overline{N}_{\rm cm}(\omega/T_i,\omega/T_e)=\overline{N}_{\rm cm}(\omega/T_{\rm mode}),$$

and attempting to understand the temperature distribution in the coupled modes. The coupled modes cm_h replace each hot-electron mode by some what less hot cm mode at a temperature $T_{\rm mode}$, made up of a mixture of (hot) electron-density fluctuations and (cold) ion-density fluctuations. Similarly the cold-ion modes are replaced by less cold cm modes cm_c. The energy relaxation between cm_h and cm_c is less efficient than the unrenormalized hot-electron modes and cold-ion modes. However, it is not easy to determine whether such coupled modes are important or not in dense plasmas, and what their relevant time scales are, at the present stage of our research. The coupled-mode problem is a nonlinear effect going beyond the first-order Fermi golden rule result, and at this stage we have no clear understanding of other nonlinear effects and the time scales required for the coupled-mode picture to survive. However, there is no question that the FGR result by itself predicts a much slower energy relaxation of hot electrons in dense plasmas than had been anticipated on the basis of Spitzer-like approaches. Some of the recently available experimental results do seem to favor relaxation-rate constants which are about an order of magnitude smaller than anticipated [18,19]. However, the analysis of the experimental data needs more careful and case-specific calculations.

TABLE II. Calculated values of the electron-ion coupling constant $\overline{g}_{\rm cc}$ for Al at normal density, and with $T_i = 0.081\,26$ eV. Results from the Spitzer-Brysk (SB), Fermi golden rule (FGR), and coupled mode (CM) calculation are given in W/K/cubic meter.

T (eV)	SB/10^{20}	FGR/10^{17}	CM/10^{16}
3.0	0.04972	0.1691	0.1744
4.0	0.09383	0.1795	0.2048
5.0	0.1467	0.1918	0.2294
7.0	0.2603	0.2050	0.2475
9.0	0.3422	0.2460	0.2416
10.0	0.3634	0.3337	0.2374
15.0	0.4234	0.2957	0.2994
20.0	0.5099	0.3538	0.3157
25.0	0.5816	0.4372	0.3336
30.0	0.6675	0.5111	0.3456
35.0	0.7688	0.7405	0.3416
40.0	0.8850	1.4210	0.2816

In this paper we have presented results for a system of hot electrons and cold ions. The case of cold electrons and hot ions involves a different set of calculations where the high-temperature ion-structure factors, etc., have to be calculated using pair potentials constructed from pseudopotentials screened by cold electrons. Although the electrons are cold, they can still follow the ion motion, and hence electronic self-consistent field calculations will be needed in setting up the quasi-EOS. Another interesting problem is the case where the hot-electron distribution has a super-high-temperature ''spike'' imposed on the underlying distribution at T_e. These issues will be taken up in future work using the same formal methods.

IV. CONCLUSION

The results presented show that the usual Spitzer-Brysk-type calculation badly overestimates the FGR result in the regime studied here. The collective nature of charged fluids is ignored in the Spitzer-Brysk form. The extremely weak overlap between the spectral functions of the electron-density fluctuation (plasmonlike) and ion-density fluctuation (acoustic excitations) is the cause of the extremely slow energy exchange between the two subsystems. The inclusion of coupled-mode effects leads to a further decrease of the relaxation rate, and it is entirely possible that mode-coupling effects could be quite important in many dense-plasma situations. Currently available time-resolved experimental methods would be able to probe the interplay of time scales, mode coupling, mode damping, and other fascinating aspects of nonequilibrium dynamics of these systems, and obtain realistic values of the energy-relaxation coupling constants. Just as theory can guide certain experimental investigations, nonequilibrium statistical theory urgently needs good experimental sign posts to guide its further development.

ACKNOWLEDGMENTS

We acknowledge many discussions with Andrew Ng and his co-workers at the University of British Columbia in the

course of this work. We thank Hugh deWitt for drawing our attention to Ref. [20].

APPENDIX A: THE QUASIEQUATION OF STATE

In this appendix we review the concept of a ''quasiequation of state'' for a two-temperature plasma in a steady state. If the ion subsystem and the electron subsystem are assumed to be completely independent (i.e., ignoring the ion-electron interaction term, giving no energy relaxation or coupled modes), then a fully decoupled treatment is easily carried out [20]. In reality, the main difficulty is to include the interaction part of the Hamiltonian for which a single temperature cannot be assigned. Further, the usual statistical mechanical approaches (at equilibrium) require a coupling-constant integration over the interactions in obtaining thermodynamic quantities. In the work of Boercker and More, the validity of their assumed Eq. (1.1) was not examined (say, using Zubarev or Keldysh methods). Their Eq. (1.1) arbitrarily selected a temperature for the electron-ion interaction $V_{\rm ei}$ which is included in the partition function. They treat the electron-ion interaction only to second order. The ions are assumed to be point ions of fixed charge to be determined by some other theory. The electrons are also assumed to be *classical*. In reality, the two-temperature quasi-equation-of-state has to address quantum electrons which form bound states in a manner different from an equilibrium plasma, and leads to an ionization balance which has to be explicitly calculated for the given T_e and T_i. Boercker and More present expressions for the dynamic structure factors (in the classical limit), but their numerical computability is not demonstrated and they are not used in subsequent theory. Note that our dynamic structure factors are ''all order'' in the electron-ion interaction, in that the pseudopotentials were constructed from all electron calculations sorting out the bound states and phase-shifted continuum states. Borecker and More did not use their dynamic structure factors to discuss electron-ion equilibriation. They used single-particle theory (''stopping-power arguments''), and presented a hand made recipe for extending the Coulomb logarithm to strong-coupling plasmas.

These difficulties (i.e., inclusion of bound-state formation, strong ion-ion coupling, nonequilibrium effects, and quantum effects) can be overcome within a certain approximate point of view (quasiequilibrium density matrix in the sense of Zubarev) if we suitably generalize the method given by us for the first principles calculation of the EOS. There we used a density-functional approach where the interacting systems are replaced by noninteracting Kohn-Sham systems made up of electrons and neutral pseudoatoms. To the extent that the effect of one subsystem with its interactions, fluxes and currents could be regarded as providing an external potential to the other subsystem, a Mermin-Kohn-Sham-type treatment can be applied to each subsystem, even though the two subsystems *taken together* are not in equilibrium. Hence we write the quasifree energy per ion of the total system as

$$F = F_{\rm id} + F_{\rm eg} + F_{\rm em} + F_{\rm xs}. \tag{A1}$$

The first term is the ideal ion-fluid contribution, and depends only on the ion temperature T_i, ion mass M, and the ion density $\bar{\rho}$. Here $F_{\rm eg}$ is the free energy of the electron gas inclusive of electron-electron interactions, and depends only on T_e, and the electron density $\bar{n}$. Hence this too can be unambiguously evaluated [1]. The remaining two terms $F_{\rm em}$ and $F_{\rm xs}$ are the energy of ''embedding'' the ions in the electron gas, and the excess free energy of the fluid. Both these terms involve the interaction term of the Hamiltonian and require some care in the nonequilibrium situation. It turns out that in the calculation of $F_{\rm em}$ for a single ion we invoke the ion temperature and ion density only to define the Wigner-Seitz cavity for placing the nucleus of the ion. The nucleus and the cavity are now placed in the electron gas at a temperature T_e, and the Kohn-Sham procedure is carried out. Thus in this calculation also, no formal problems arise and the conditions for the applicability of the Mermin-Kohn-Sham procedures hold. Similarly, this calculation provides us with the electron charge displacement around each ion, and hence the pseudopotential $U_{\rm ie}(T_e)$ for the ion at the electron temperature T_e. However, if the experiment is such that the *initial state* of the system determines the ion distribution function and if this remained essentially unchanged during the short laser pulse, then we need $U_{\rm ie}(T_i)$, i.e., at the *ion temperature*, to determine the ion-ion pair potential that determines the ion distribution. Thus the excess free energy of the fluid can be evaluated via HNC equations as in Ref. [1], and $F_{\rm xs}$ entering into the quasi-EOS is the $F_{\rm xs}$ evaluated at T_i.

Once the expression for the quasi-EOS free energy has been written down, there is no overall free-energy minimum principle that can be invoked to evaluate the ion-species compositions, etc. However, when the time scales of the problem are such that the ion subsystem remains unchanged, all the ion-composition parameters retain their initial value within the given time step. On the other hand, the electron time scales are assumed to be quite short in comparison to the time step, and hence we *can* minimize the expression for the quasi-EOS free energy with respect to the electron density $\bar{n}$, subject to the constrain of overall charge neutrality. If we consider a single-species fluid or an average-atom model, this simply means that $\bar{n}$ variations are exactly compensated for by changes in the degree of ionization $\bar{Z}$. Further, a Kohn-Sham equation rigorously exists whenever the variation with respect to $\bar{n}$ is legitimate within the given time scales.

APPENDIX B: KELDYSH TECHNIQUE FOR COUPLED ELECTRON-ION MODES

The standard Keldysh method deals with a single-temperature density matrix and its evolution (possibly to a two-temperature steady state, etc.) in time. The analysis using a two-temperature model from the outset is less clear, but we assume that the quasiequilibrium density matrix of Zubarev [5] can be employed to justify the approach. Also, the more formal issues of the existence of a Wick theorem, etc., were discussed by Lei and Wei [21]. The diagram of Fig. 3(a) shows an electron-polarization fluctuation loop with the vertices connected by the ion-electron interaction $U_{\rm ie}(q)$. When coupled modes are formed, this interaction itself ac-

quires insertions of the electron-polarization loop, and a new vertex function $\tilde{\Lambda}(q,\omega)$ is generated. We distinguish the 2×2 Keldysh matrix Green functions by placing a tilde on the Green functions, etc., as in $\tilde{G}$. Thus the electron Green function $\tilde{G}$ and the ion-density Green function $\tilde{B}$ are [22]

$$\tilde{G}=\begin{pmatrix} g^r & \overline{g} \\ 0 & g^a \end{pmatrix} \quad \text{and} \quad \tilde{B}=\begin{pmatrix} b^r & \overline{b} \\ 0 & b^a \end{pmatrix},$$

where the superscripts r and a denote the retarded and advanced functions. The overbars on g and b indicate a correlation function. The electron propagators have the form

$$g^{r,a}(k,\omega)=(\omega-\epsilon_k\pm i\gamma_e)^{-1},$$

$$\overline{g}(k,\omega)=[1+2N(\omega/T_e)]^{-1}(g^r-g^a).$$

For brevity of presentation, we take the ion-density fluctuation propagators to have a single mode (e.g., an ion-plasmon mode or an ion-acoustic mode with an excitation energy ω_q). Then the analysis becomes analogous to the problem of electrons interacting with a single phonon mode [24]. We have

$$b^r=(b^a)^*=(\omega-\omega_q+i\gamma_i)^{-1}-(\omega+\omega_q+i\gamma_i)^{-1},$$

$$\overline{b}=[1+2N(\omega/T_i)](b^r-b^a).$$

The convolution of an electron propagator with a hole propagator gives the electron-density-fluctuation loop, and we denote its iteration by χ_e. Then the matrix-vertex function $\tilde{\Lambda}(q,\omega)$ describing the electron-ion interaction is of the form $\tilde{\Lambda}=\left(\begin{smallmatrix} \lambda^r & \overline{\lambda} \\ 0 & \lambda^a \end{smallmatrix}\right)$, where

$$\lambda^r(\omega)=|U_{\rm ie}(q)|^2\ \mathrm{Im}\chi_e(q,\omega),$$

$$\lambda^a(\omega)=\lambda^r(-\omega),$$

$$\overline{\lambda}=-2|U_{\rm ie}(q)|^2\ \mathrm{Im}\chi_e(q,\omega)[11+2N(\omega/T_e)].$$

The matrix Dyson equation defining coupled-mode formation is

$$\tilde{B}_{\rm cm}=\tilde{B}+\tilde{B}\tilde{\Lambda}\tilde{B}_{\rm cm}. \tag{B1}$$

The expressions for the coupled-mode propagators are thus seen to be

$$b_{\rm cm}(q,\omega)=b^r(q,\omega)/W(q,\omega),$$

$$\overline{b}_{\rm cm}=[\overline{b}+|b^r|^2\overline{\lambda}]/|W|^2,$$

$$W=1-b^r|U_{\rm ie}(q)|^2\mathrm{Im}\chi_e(q,\omega).$$

The correlation function $\overline{b}_{\rm cm}$ provides the coupled-mode distribution function. The energy relaxation rate is obtained by evaluating Fig. 2(b) using the expressions for the cm Green functions given above and the standard diagram rules [4]. Thus

$$\dot{E}_e=\Sigma|U_{\rm ie}(q)|^2\int\frac{d\omega\nu}{(2\pi)^2}\omega\ \mathrm{Tr}[Z_{\kappa\kappa'}(k,q,\omega,\nu)\tilde{B}_{\rm cm}^{\kappa\kappa'}(q,\omega)],$$

$$Z_{\kappa\kappa'}=\overline{\gamma}^{\kappa}\overline{G}(k,\nu)\tau^1\gamma^{\kappa'}\tilde{G}(\mathbf{k}-\mathbf{q},\nu-\omega).$$

Here γ and $\overline{\gamma}$ are 2×2 matrices expressed in terms of the Pauli matrixes τ and defined by Rammer and Smith [4]. Using the random-phase-approximation form for the electron term and evaluating the ν integration, we obtain the energy-relaxation rate given in Eq. (50).

[1] F. Perrot and M. W. C. Dharma-wardana, Phys. Rev. E **52**, 5352 (1995).

[2] L. Spitzer, *Physics of Fully Ionized Gases* (Interscience, New York, 1962). We have referred to ''Spitzer-type'' calculations, even though many of them were developed by the Landau school as well. See Ref. [4].

[3] H. Brysk, Plasma Phys. **16**, 927 (1974).

[4] P. C. Martin and J. Schwinger, Phys. Rev. **115**, 1342 (1959); J. Rammer and H. Smith, Rev. Mod. Phys. **58**, 323 (1986); L. D. Landau and E. M. Lifshitz, *Course in Theoretical Physics* (Pergamon, Oxford, 1981), Vol. 10, Chap. X.

[5] D. N. Zubarev, *Non-Equilibrium Statistical Thermodynamics* (Consultants Bureau, New York, 1974).

[6] Y. T. Lee and R. M. More, Phys. Fluids **27**, 1273 (1984).

[7] S. Ichimaru, *Basic Principles of Plasma Physics* (Benjamin, London, 1973).

[8] A. Ng, P. Celliers, G. Xu, and A. Forsman, Phys. Rev. E **52**, 4299 (1995).

[9] A. Fetter and J. Walecka, *Quantum Theory of Many-Particle Systems* (McGraw-Hill, New York, 1971); G. D. Mahan, *Many-Particle Physics* (Plenum, New York, 1981).

[10] M. W. C. Dharma-wardana and F. Perrot, *Density Functional Theory*, edited by E. K. U. Gross and R. M. Dreizler (Plenum, New York, 1995); N. D. Mermin, Phys. Rev. **137**, A1441 (1965); P. Hohenberg and W. Kohn, Phys. Rev. **136**, B864 (1964); W. Kohn and L. J. Sham, Phys. Rev. **140**, A1133 (1965).

[11] Sh. M. Kogan, Fiz. Tverd. Tela (Leningrad) **4**, 2474 (1963) [Sov. Phys. Solid State **4**, 1813 (1963)].

[12] F. Perrot and M. W. C. Dharma-wardana, Phys. Rev. A **30**, 2619 (1984); H. Iyetomi and S. Ichimaru, *ibid.* **34**, 433 (1986); D. G. Kanhere, P. V. Panat, A. K. Rajagopal, and J. Callaway, *ibid.* **33**, 490 (1986).

[13] F. Nardin, G. Jacucci, and M. W. C. Dharma-wardana, Phys. Rev. A **37**, 1025 (1988).

[14] A. Ng, D. Parfeniuk, P. Celliers, L. Da Silva, R. M. More, and Y. T. Lee, Phys. Rev. Lett. **57**, 1595 (1986); H. M. Milchberg, R. R. Freeman, S. C. Davey, and R. M. More, *ibid.* **61**, 2364 (1988).

[15] F. Perrot and M. W. C. Dharma-wardana, Phys. Rev. A **36**, 238 (1987).

[16] M. W. C. Dharma-wardana and G. C. Aers, Phys. Rev. B **28**, 1701 (1983).

[17] Yoshio Waseda, *The Structure of Non-Crystalline Materials*

(McGraw-Hill, New York, 1980).
[18] P. B. Corkum, F. Brunel, N. K. Sherman, and T. Srinivasan-Rao, Phys. Rev. Lett. **61**, 2886 (1988).
[19] P. Celliers, A. Ng, G. Xu, and A. Forsman, Phys. Rev. Lett. **68**, 2305 (1992).
[20] D. B. Boercker and R. M. More, Phys. Rev. A **33**, 1859 (1986).
[21] X. L. Lei and M. W. Wei, Mod. Phys. Lett. B **42**, 1574 (1990).
[22] We use the 2×2 matrix notation of Ref. [4], Eq. (2.27), which is slightly different from that of L. D. Landau and E. M. Lifshitz, *Course in Theoretical Physics* (Ref. [4]).
[23] D. Y. Xing and C. S. Ting, Phys. Rev. Lett. **72**, 2812 (1994), and related references given therein.
[24] M. W. C. Dharma-wardana, Solid State Commun. **86**, 83 (1993).